



POLİTEKNİK DERGİSİ

JOURNAL of POLYTECHNIC

ISSN: 1302-0900 (PRINT), ISSN: 2147-9429 (ONLINE)

URL: <http://dergipark.org.tr/politeknik>



Utilization of CFD for the aerodynamic analysis of a subsonic rocket

Hesaplamaalı Akışkanlar Dinamiği ile ses altı bir roketin aerodinamik analizi

Yazarlar (Authors): Zeynep AYTAÇ¹, Fatih AKTAŞ²

ORCID¹: 0000-0003-0717-5287

ORCID²: 0000-0002-1594-5002

Bu makaleye şu şekilde atıfta bulunabilirsiniz (To cite to this article): Aytaç Z. ve Aktaş F., "Utilization of CFD for the aerodynamic analysis of a subsonic rocket", *Politeknik Dergisi*, 23(3): 879-887, (2020).

Erişim linki (To link to this article): <http://dergipark.org.tr/politeknik/archive>

DOI: 10.2339/politeknik.711003

Hesaplamalı Akışkanlar Dinamiği ile Ses Altı Bir Roketin Aerodinamik Analizi

Araştırma Makalesi / Research Article

Zeynep AYTAÇ*, Fatih AKTAŞ

Mühendislik Fakültesi, Makine Müh. Bölümü, Gazi Üniversitesi, Ankara, Türkiye

(Geliş/Received : 29.03.2020 ; Kabul/Accepted : 07.04.2020)

ÖZ

Günümüzde her ülke, kendi yerli ve milli savunma sanayisini geliştirmeyi hedeflemektedir. Bu doğrultuda, füze ve roket gibi yapıların tasarımı çok daha önemli hale gelmiştir. Bu çalışmada, Hesaplamalı Akışkanlar Dinamiği (HAD) yardımıyla, ses altı hızda bir roketin tasarımı ve aerodinamik analizleri gerçekleştirilmiştir. Ayrıca, Mach sayısı, türbülans yoğunluğu, ve türbülans modeli gibi kritik parametrelerin roket performansına etkileri incelenmiştir. Çalışma sonucunda, Mach sayısının sürüklenme katsayısı üzerinde ciddi bir etkiye sahip olduğu görülmüştür. Mach sayısındaki %30'luk bir artış, sürüklenme katsayısının yaklaşık olarak %68 artmasına sebep olmuştur. Bunun tersine, türbülans yoğunluğunun değiştirilmesinin ise sürüklenme katsayısında belirgin bir farka sebep olmadığı görülmüştür. Her ne kadar, her problem özelinde uygun türbülans yoğunluğu kullanımının önemli olduğu bilirse de, mevcut problem için türbülans yoğunluğu seçiminin zaman harcanacak bir kriter olmadığı sonucuna varılmıştır. Son olarak, türbülans modeli seçiminin, beklendiği gibi, tasarım açısından oldukça önemli olduğu görülmüştür. Benzer problemlerin çözümü için literatürde yaygın olarak kullanılan $k-\omega$ SST ve diğer bir model olan $k-\omega$ arasında, sürüklenme katsayısı açısından yaklaşık %12 fark olduğu görülmüştür. Beklendiği gibi, $k-\omega$ modelinden elde edilen sonuç, $k-\omega$ SST modelinden elde edilen sonuçtan daha yüksektir.

Anahtar Kelimeler: Roket, Hesaplamalı Akışkanlar Dinamiği, tasarım metodolojisi, ses altı akış, dış akış.

Utilization of CFD for the Aerodynamic Analysis of a Subsonic Rocket

ABSTRACT

Nowadays, every single country aims to have a domestic and national defense industry. In accordance with this purpose, the design of missile structures has become more important than ever. In this study, the design and analyses of a subsonic rocket was carried out with the utilization of Computational Fluid Dynamics (CFD) tools. Also, the effects of several critical parameters; i.e. Mach number, turbulence intensity, turbulence model, on the rocket performance were investigated. It was found out that a variation in Mach number has a substantial effect on the drag coefficient; i.e. an increment in Mach number at approximately 30% results in an increment of drag coefficient nearly 68%. Contrarily, changing the turbulence intensity does not make any significant difference on drag coefficient. Although the appropriate turbulence intensity should be used for every unique problem, in this case, this parameter is not a critical variable to ponder upon. Finally, the implementation of the appropriate turbulence model is critical in the design process as expected. Utilization of $k-\omega$ and $k-\omega$ SST models differs approximately 12% in terms of drag coefficient; the drag coefficient obtained from $k-\omega$ is higher than that of obtained from $k-\omega$ SST.

Keywords: Rocket, Computational Fluid Dynamics, design methodology, subsonic flow, external flow.

1. INTRODUCTION

Today, with the developing political strategies and relationships, each country attaches particular importance to their defense industry. Similarly, Turkey aims to design and manufacture its own missiles. In accordance with this purpose, the know-how of the design process of these structures started to develop and became widespread than ever.

Rockets are used for various purposes in defense and research industry. They carry payloads into the orbit or space, or they can be used for weapon applications. The first rocket in history is designed and manufactured in China in 1200 and used as fireworks during the New Year celebrations [1]. A body immersed in a fluid medium

exposes aerodynamic forces resulting from the relative motion between the body and the fluid [2]. Rocket aerodynamics defines the structure of the air flow through a rocket and it presents the effect of this flow on drag and stability. The main purpose of the designer is to find out the optimal shape provides the required specifications with the design criterions with the minimum cost and fuel consumption [3]. More specifically, one should minimize the drag force with a maintained stability whereas he/she should predict the thrust and optimize the fuel utilization. Stability expresses a rocket's ability to fly through the air aiming the right point in the right trajectory without any deterioration.

Basically, a rocket structure consists of two main components; the airframe and the internals. The airframe part is made up of nose cone, body tube and fins whereas

*Sorumlu Yazar (Corresponding Author)
e-posta : fzaytac@gmail.com.tr

the internals are parachutes and shock cord, electronic accessories and motor. Figure 1 represents the structure of a rocket.

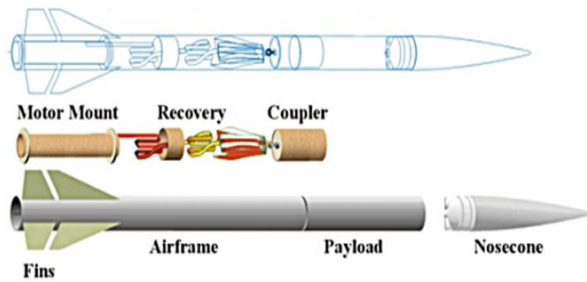


Figure 1. The rocket structure [4]

The nosecone splits the airflow around the vehicle which maintains the speed and each nosecone has a unique structure designed for that specific airflow and vehicle. The amount of air resistance that the vehicle experiences depends mainly on the shape of the nose cone, the body diameter and the speed. For subsonic applications, it is known that a rounded curved nosecone shape is more beneficial. The body cylinder keeps the pressure distribution even throughout the vehicle and it constitutes the main structure of the rocket. The larger the diameter of the body gets, the more drag force that the vehicle is exposed to. In addition, it provides a safe housing for the internal components. The fins are required for the stability of the vehicle, even if they cause the drag force to increase. These components should be designed optimally to fulfil the mission successfully [5]. Generally, the rocket structures are symmetrical with respect to their center line passing through its nose and body, providing several simplifications in terms of aerodynamic design process [6]. The aerodynamic design of a missile vehicle should be performed precisely whether it has a subsonic, supersonic, sonic or transonic flow regime [7].

The airflow characteristics such as airflow velocity, flow rate, pressure, drag force, etc. affect substantially the exterior ballistics of the rocket [8]. The aerodynamic coefficients, which are drag and lift coefficients, are dimensionless quantities which are used to determine the aerodynamic characteristics of a structure. They are determined by the ratio of several forces, rather than just the forces themselves. The aerodynamic forces result primarily from the differences in pressure and viscous shearing stresses [2].

The drag coefficient of a structure is used to model the drag of a body immersed in a fluid medium. The drag coefficient is the most critical parameter for the investigation of exterior ballistics. Consequently, the rocket engine thrust characteristics are directly influenced by this specific parameter. It depends on the shape of the structure, inclination and the flow condition and it is expressed with Equation 1.

$$C_D = \frac{2F_D}{\rho AV^2} \quad (1)$$

Here, C_D presents the drag coefficient, F_D represents the drag force, ρ the density, A the cross-sectional area of the body and V the speed. As the drag coefficient gets smaller, one can understand that the structure experiences a less aerodynamic drag.

Similarly, the lift coefficient expresses the ratio of the lift force to the force resulting from the multiplication of dynamic pressure to the area. Lift force is the force which is perpendicular to the oncoming flow direction. For a lift force to be generated, a pressure difference between the upper and lower sides of the structure is required.

1.1. Utilization of CFD for Aerodynamic Design of a Rocket

The design process of a rocket with experimental processes and measuring all the necessary variables in wind tunnels can be exhausting, time and money consuming for most researchers [9]. A reasonable prediction of these parameters with the utilization of appropriate approaches is offered by CFD simulations. Today, with the advances and conveniences in computer technology and computational tools led CFD to become an essential design tool, reducing the costs of experimental studies [10]. CFD tools enable accurate solutions to complex, three-dimensional problems for missile aerodynamics [11]. When the problem is formed using the right numerical models and approaches, CFD offers qualified information that can be derived routinely for a wide range of applications [12]. It is widely used in aeronautical applications during the conceptual and preliminary design stages, as it reduces the design cycle time and minimizes the expenses related with the experimental procedures [13,14,15].

1.2. Specifications of the Rocket

The dimensions of the designed rocket are given in Figure 2. The specified dimensions are given in millimeters.

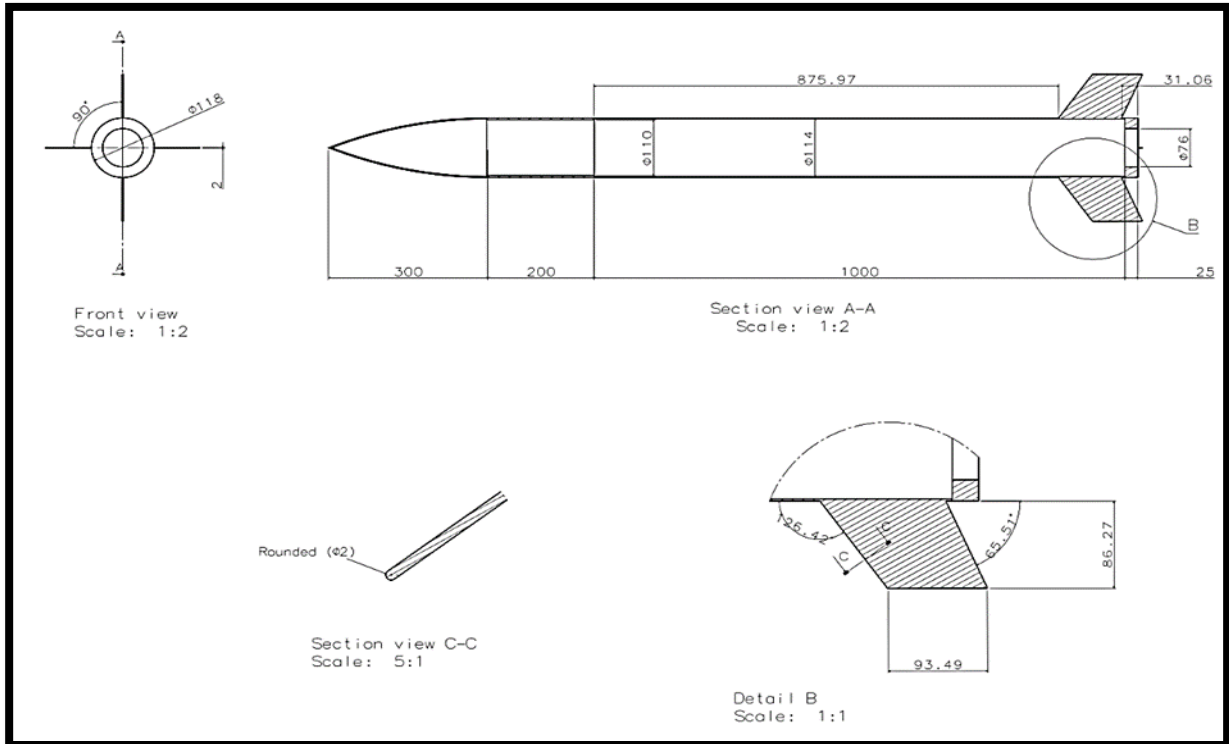


Figure 2. The dimensions of the designed rocket

In addition, the rocket is required to operate at atmospheric conditions (1 atm, 25°C) with a maximum velocity of 170 m/s.

2. METHODOLOGY

Each missile structure has a unique design depending on its requirements. As mentioned above, as the experimental process is infeasible in many ways, Computational Fluid Dynamics becomes a prominent tool at this point. In the present study, traditional CFD methodology was followed in order to simplify the design process. The outline is given in Figure 3.

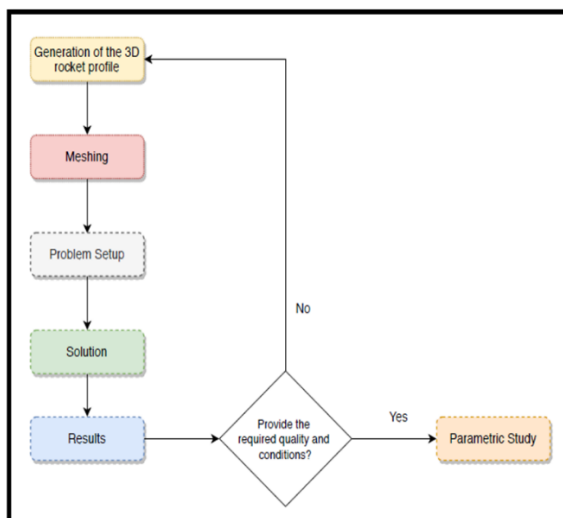


Figure 3. The design methodology

2.1. 3D Modeling

Initially, the 3D model of the missile was created using CATIA in the light of dimensional specifications. The generated model is given in Figure 4.

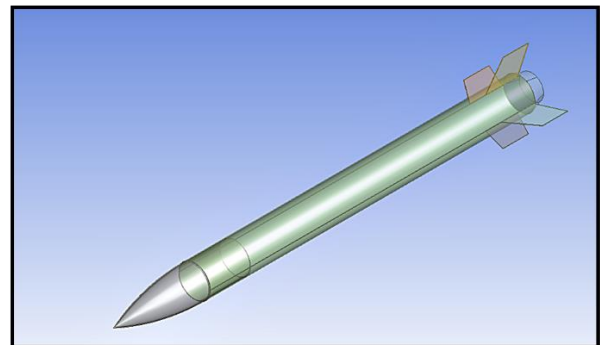


Figure 4. The 3D model of the designed rocket

2.2. Grid Generation

After the geometry generation, the 3D model of the rocket was meshed using ANSYS Meshing. A high-quality mesh is critical to provide the accuracy and stability of a numerical solution [2]. So, the grid structure should be constructed neatly in order to successfully represent the physical phenomena in the flow domain. Here, it is known that the boundary layer resolution at the top of the body is of substantial importance. In addition, inlet and outlet regions constitute the other locations to pay attention on. Also, as this problem requires the determination of drag force, the boundary layer is required to have a fine mesh structure.

The generated grid structure is given in Figure 5.

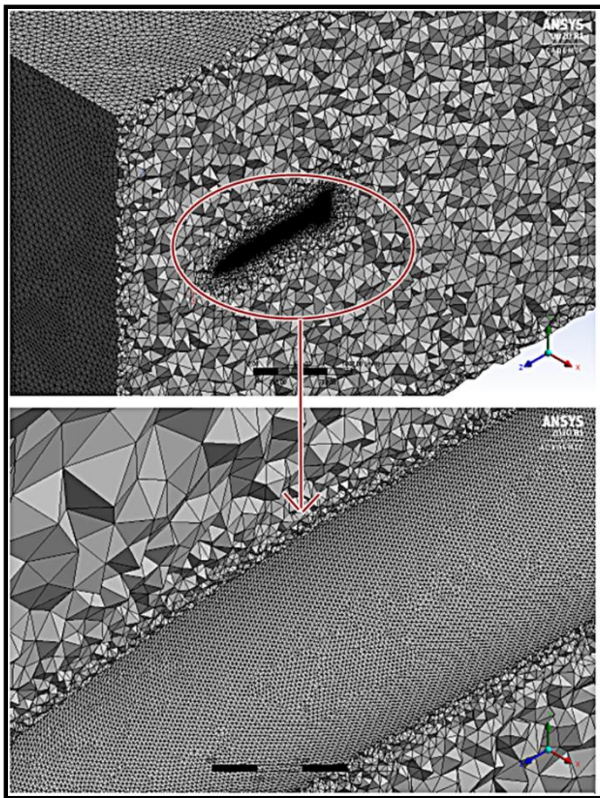


Figure 5. The generated mesh structure

As it can be seen from Figure 5, the region surrounding the rocket profile has a denser mesh structure, whereas the density of the mesh is decreasing as one progresses through the boundary of the domain. This structure is constructed by using inflation layers. The first layer thickness of the inflation layer is 0.0018 mm. This parameter is kept as small as possible so that the first layer is located close to the rocket body [8]. It is mentioned above that this structure is necessary in order to successfully resolving the boundary layer.

The detail of mesh statistics is given in Figure 6.

Display	
Defaults	
Sizing	
Quality	
Check Mesh Quality	Yes, Errors
<input type="checkbox"/> Target Skewness	Default (0.900000)
Smoothing	
Mesh Metric	Skewness
<input type="checkbox"/> Min	1,3278e-008
<input type="checkbox"/> Max	0,90102
<input type="checkbox"/> Average	0,17344
<input type="checkbox"/> Standard Deviation	0,13368
Inflation	
Assembly Meshing	
Advanced	
Statistics	
<input type="checkbox"/> Nodes	2991459
<input type="checkbox"/> Elements	10193109

Figure 6. Mesh statistics

The skewness value represents the difference between the shape of a cell and the shape of an equilateral cell of equivalent volume. So, this value is needed to be minimized in fine mesh structures. A general rule for most flows that the skewness is below 0.95, with an average value of much lower [2]. The generated structure in this study has a maximum skewness of 0.9 and an average skewness of 0.17344. In other words, the grid structure stays on the safe side.

Figure 7 represents the mesh metrics in terms of skewness.

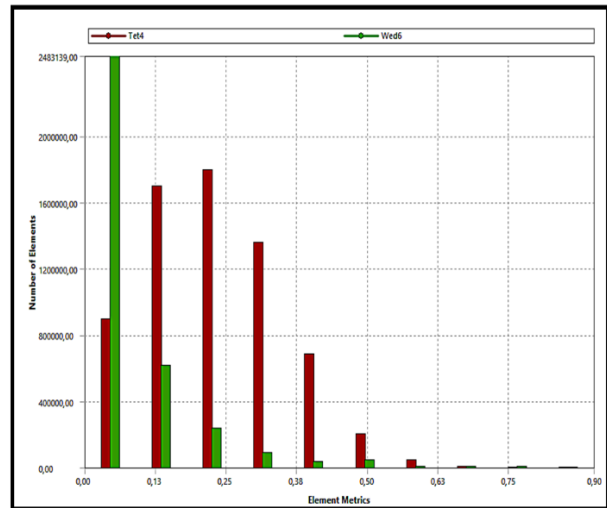


Figure 7. Mesh metrics

It can be seen from Figure 5 that most of the elements have a skewness of 0.5 or lower. Only a minority of them have a skewness value larger than 0.5, which are the ones located near the fins. This is a result of the sharp corners and edges of the fin profile, obstructing the smooth transition of the mesh cells.

Finally, in order to ensure that the results are independent of the mesh structure, a mesh independency study was carried out. The results are compared with respect to the drag force calculated. The results are given in Table 1.

Table 1. Results of the mesh independency study

Element Number [x10 ³]	Drag Force [N]
13500	77.2
10100	77.05
9200	77.06
5800	78.48
5600	78.65
1600	78.9
635	84.02

Even decreasing the mesh number by half; from 13.5M to 5.8M, does not create a difference more than 2%. So, rather than using 13.5M elements, it is more feasible to

use 5.8M elements to save from computational time and resources.

2.3. Solver Settings and CFD Analyses

To model the 3D motion of a fluid particle, Navies-Stokes equations are used. The equations are given in the following subsections.

2.3.1. Conservation of Mass

The mass conservation for a particle having dimensions of dx, dy and dz is expressed with Equation 2.1.

$$\frac{\partial \rho}{\partial t} + \frac{\partial(\rho u_i)}{\partial x_i} = 0 \quad (2.1)$$

x - component:

$$\begin{aligned} \rho \frac{D\bar{u}}{Dt} &= \rho \left[\frac{\partial}{\partial x} (\bar{u}^2) + \frac{\partial}{\partial y} (\bar{u}\bar{v}) + \frac{\partial}{\partial z} (\bar{u}\bar{w}) \right] \\ &= \rho g_x - \frac{\partial \bar{P}}{\partial x} + \frac{\partial}{\partial x} \left[\mu \frac{\partial \bar{u}}{\partial x} - \rho \overline{u'^2} \right] + \frac{\partial}{\partial y} \left[\mu \frac{\partial \bar{u}}{\partial y} - \rho \overline{u'v'} \right] + \frac{\partial}{\partial z} \left[\mu \frac{\partial \bar{u}}{\partial z} - \rho \overline{u'w'} \right] \end{aligned}$$

y - component:

$$\rho \frac{D\bar{v}}{Dt} = \rho \left[\frac{\partial}{\partial x} (\bar{u}\bar{v}) + \frac{\partial}{\partial y} (\bar{v}^2) + \frac{\partial}{\partial z} (\bar{v}\bar{w}) \right] = \rho g_y - \frac{\partial \bar{P}}{\partial y} + \frac{\partial}{\partial x} \left[\mu \frac{\partial \bar{v}}{\partial x} - \rho \overline{u'v'} \right] + \frac{\partial}{\partial y} \left[\mu \frac{\partial \bar{v}}{\partial y} - \rho \overline{v'^2} \right] + \frac{\partial}{\partial z} \left[\mu \frac{\partial \bar{v}}{\partial z} - \rho \overline{v'w'} \right] \quad (2.3)$$

z - component:

$$\begin{aligned} \rho \frac{D\bar{w}}{Dt} &= \rho \left[\frac{\partial}{\partial x} (\bar{u}\bar{w}) + \frac{\partial}{\partial y} (\bar{v}\bar{w}) + \frac{\partial}{\partial z} (\bar{w}^2) \right] \\ &= \rho g_z - \frac{\partial \bar{P}}{\partial z} + \frac{\partial}{\partial x} \left[\mu \frac{\partial \bar{w}}{\partial x} - \rho \overline{u'w'} \right] + \frac{\partial}{\partial y} \left[\mu \frac{\partial \bar{w}}{\partial y} - \rho \overline{v'w'} \right] + \frac{\partial}{\partial z} \left[\mu \frac{\partial \bar{w}}{\partial z} - \rho \overline{w'^2} \right] \end{aligned}$$

2.3.3. Turbulence Model

Although the Navier-Stokes equations are simplified with the conservation equations and the averaging procedure, it is still not possible to solve them analytically. So, the two-equations coming from the turbulence model are required in order to solve the flow accurately. The present study uses k- ω SST model in addition to RANS equations. This model is the most suitable model for aeronautics applications where strong adverse pressure gradients and separation are observed. Although standard k - ω model over predicts separation, k - ω SST comes through this problem. The utilization of k- ω SST makes the model directly usable from the boundary layer region all the way down through the viscous sublayer. This formulation switches to k- ϵ behavior within the free stream; overcoming the over predicting model.

2.4. Simulation

ANSYS CFX-Pre is used to set up the cases and ANSYS CFX Solver is used to simulate the problem. The regions used to define the boundary conditions are given in Figure 8.

2.3.2. Conservation of Momentum

Law of conservation of momentum is simply the Newton's second law of motion. It states that the time rate of change of momentum of a system is equal to the sum of external forces acting on that body and is expressed with Equation 2.2.

$$\frac{D(u_i)}{Dt} = \frac{\partial u_i}{\partial t} + u_j \frac{\partial u_i}{\partial x_j} = -\frac{1}{\rho} \frac{\partial P}{\partial x_i} + \nu \frac{\partial^2 u_i}{\partial x_j^2} + F_i \quad (2.2)$$

The external flow domain of a rocket is simulated using Reynolds Averaged Navier – Stokes (RANS) equations. RANS methods are widely used in industrial applications [16]. The equations are given in Equation 2.3, separately for x, y and z axes.

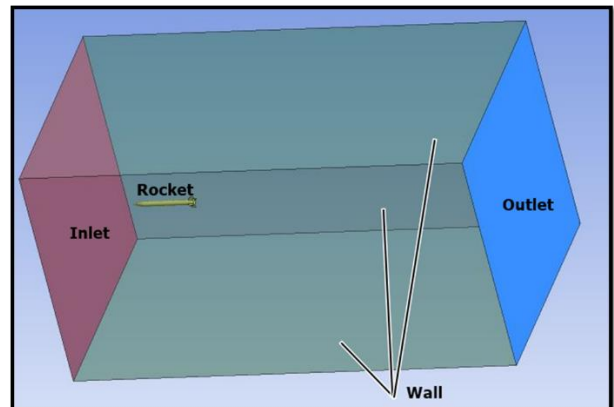


Figure 8. The regions used for setting up the boundary conditions for the CFD analyses

In Figure 8, the pink region represents the inlet, the blue represents the outlet, the green parts represent the walls. The yellow part is the rocket. The inlet and outlet locations are selected as “Inlet” and “Outlet” boundary types, respectively. The inlet boundary is defined with the normal speed, 170 m/s and the outlet boundary is defined with the static pressure, 0 Pa. The reference pressure is selected as 1 atm. The rocket is defined as a

non-slip wall and the remaining regions are selected as symmetry. The fluid is air – ideal gas and as mentioned, k- ω SST turbulence model is utilized. The residual target is specified as 10⁻⁶. Furthermore, a monitor point was used to monitor the velocity value in the middle section to check the convergence. The problem was solved using steady-state conditions.

After setting up the cases, analyses were conducted using CFX Solver Manager. The obtained results are given in Section 3.

3. RESULTS AND EVALUATION

The analyses were conducted for various Mach numbers of 0.35, 0.5 and 0.65. Also, results from several turbulence models and turbulence intensities were compared with each other. The results are given separately for each parametric analysis. The actually designed case is the one with the low intensity turbulence, 0.5 Ma and k- ω SST turbulence model.

3.1. The Design Case

The contours of pressure, total pressure, velocity, y+ and the velocity vectors are given in the proceeding figures.



Figure 9. The Mach number contour

As 170 m/s corresponds to 0.5 Ma, the enclosure region contour is red in color. According to the flow separation at the nose cone, a region of low velocity and a stagnation point is observed, and a thin boundary layer is developed at the top of the body region. At the outlet region, a region of low velocities and even zero velocity is observed. This is due to the vortex formations at the outlet, which results in flow circulations locally.

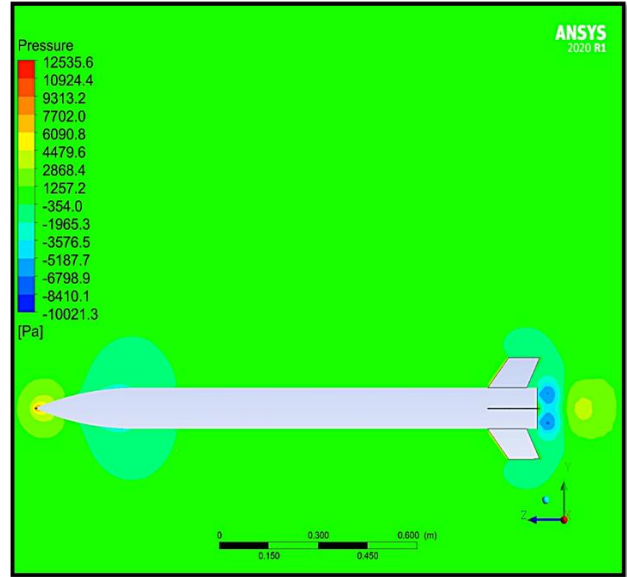
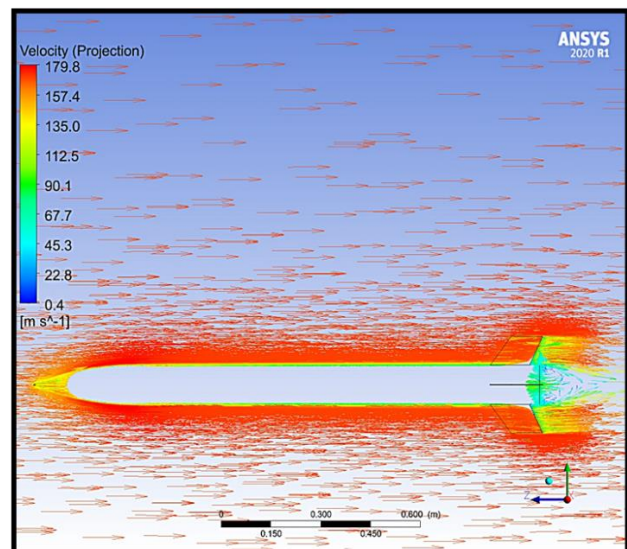


Figure 10. The pressure contour

As explained in Figure 9, there is a stagnation point in front of the nose cone. Consequently, this point has the maximum pressure. The pressure values at the top and bottom of the rocket are equal; which means that there is no lift force. This is due to the angle of attack of the rocket, 0°. Again, a thin boundary layer development can be observed.



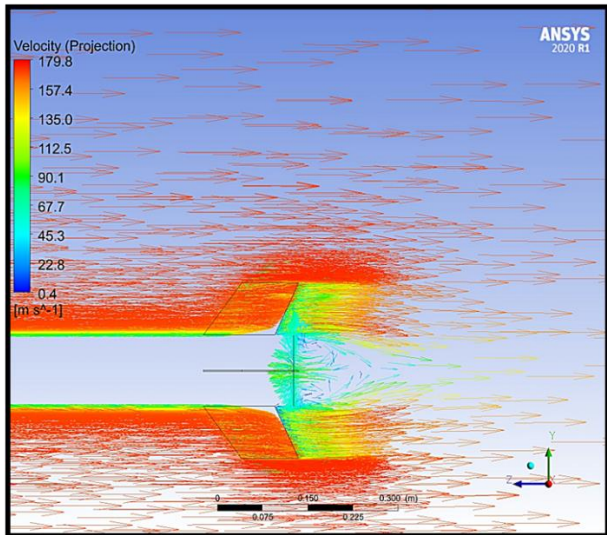


Figure 11. The velocity vectors through the flow domain and at the outlet

From Figure 11, it can be seen that the velocity contours exhibit a homogeneous direction, through the inlet to the outlet. The developed boundary layer can be seen more clearly, and the recirculation region at the back region of the rocket is obvious. In this location, because of the recirculation and formed vortices, the velocity decreases substantially.

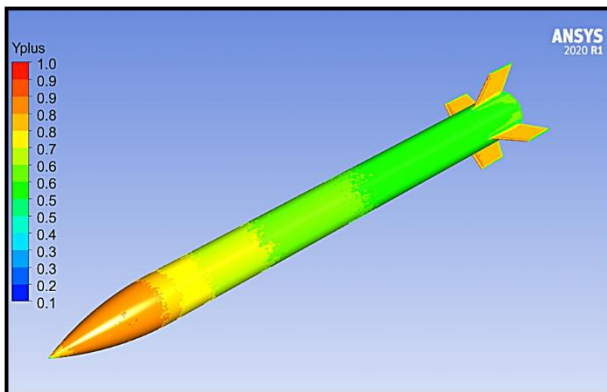


Figure 12. The y^+ contour

The y^+ value is critical in terms of accuracy of the solution. Each turbulence model requires a different range y^+ values to attain a reliable solution. y^+ simply defines the dimensionless distance from the wall which is used to check the location of the first node away from the wall [2]. As it depends on the mesh structure, it has a significant effect on the model's ability to solve the boundary layer. For the current turbulence model, this value needs to be 1 or smaller. From Figure 12, it can be seen that the maximum value of y^+ is 1.0, which are located on the fins as they have sharp edges and corners. Throughout the rest of the body, it is 0.7 or smaller; which expresses that the obtained results are accurate enough to resolve the boundary layer.

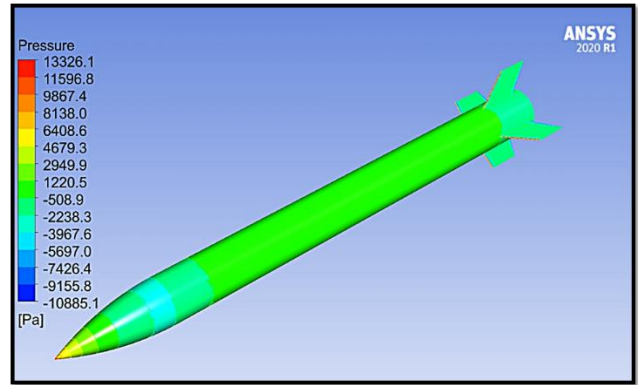


Figure 13. The pressure contour of the rocket

3.2. Parametric Study

3.2.1. Mach Number

The dependence of the results on the Mach number is investigated. Three different values of Mach numbers, 0.35, 0.5 and 0.65 are used in low intensity turbulence and $k-\omega$ SST turbulence model. The results are compared with respect to the drag coefficients obtained.

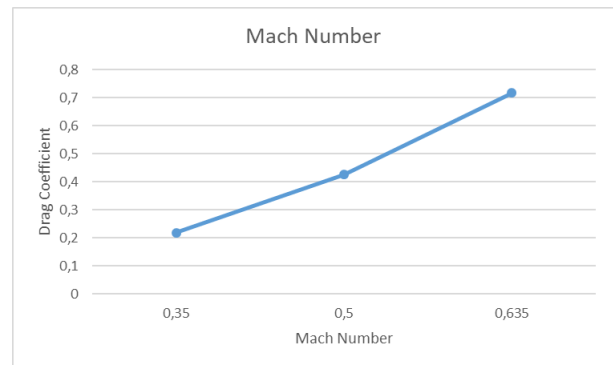


Figure 14. Mach number vs. drag coefficient

As the Mach number is increased, it can be seen that the drag force increases relatively. This is an expected result, since the increment in Mach number is equal to the increment in velocity. An increased velocity corresponds to an increased drag force, due to the increased frictional forces. An increment in Mach number at approximately 30% results in an increment of drag coefficient nearly 68%.

3.2.2. Turbulence Intensity

Turbulence intensity represents the turbulence level of the flow. It is determined depending on the previous experience on the designer and the state-of-art. Generally high turbulence level is used in high speed flows in complex geometries; such as turbomachines. The turbulence intensity is between 5% and 20% for high intensity. Medium intensity is the most common used level, as it is used for flows in not-so-complex devices or low speed flows. Its intensity varies between 1% and 5%. Low intensity is used for flows originating from a fluid which is not moving, e.g. external flow across cars, submarines and aircrafts. Low intensity has a turbulence

level lower than 1%. As this problem is typically an external flow around an air vehicle, low intensity level is used.

The results between the turbulence levels are given in Figure 15.

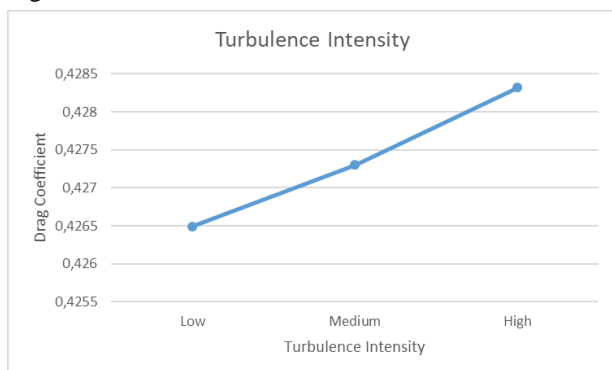


Figure 15. Turbulence intensity vs. drag coefficient

As expected, drag force increases with the increased turbulence level. However; the variation is between 77 and 77.38; which will not make quite a difference in the design process. Therefore, although the appropriate turbulence intensity should be used for every unique problem, in this case, this parameter is not a critical variable to ponder upon.

3.2.3. Turbulence Model

The specified turbulence model determines the two equations which will be solved with the RANS equations. As mentioned before, k- ω SST model was used for the design process of this case. However, the effects of several turbulence models were investigated, and the results are given in Table 2.

Table 2. Turbulence Models vs. drag force

Turbulence Model	Drag Force [N]	Drag Coefficient
BSL Reynolds	81.7362	0.452387
k- ϵ	79.6909	0.441067
k- ω	86.7081	0.479905
RNG Epsilon	78.9961	0.43722
k- ω SST	77.0578	0.42704

Accepting the result obtained from k- ω SST model as a reference, it can be seen that RNG Epsilon model is the nearest, followed by k- ϵ , BSL Reynolds and finally k- ω . One can expect k- ω model to give the nearest result to the k- ω SST model, however, k- ω model overpredicts the separation in the boundary layer, which in turn affects the drag force in a substantial manner.

4. CONCLUSION

The present study involves the design of a rocket in a subsonic speed with the utilization of CFD tools and investigates the effect of several critical parameters on the drag force; which is a reference result in rocket design processes.

It is obtained that the drag force is extremely sensitive to the variations in Mach number. A 30% increment in Mach number resulted in an increment of drag coefficient by nearly 70%.

The three turbulence intensity options existing in ANSYS CFX was used to obtain the differences in drag forces. As mentioned before, although every designer should use the correct turbulence intensity for each design problem, this case does not reveal a distinct difference between each intensity.

Finally, the available turbulence models were used to analyze the resulting drag forces. As the k- ω SST model is taken as a reference, RNG-Epsilon model gives the closest result to that of k- ω SST, then comes the k- ϵ , BSL Reynolds and k- ω models. Again, each problem has its own unique specifications and flow characteristics and turbulence model should be decided in the light of these requirements. Taking into consideration that the k- ϵ , k- ω and k- ω SST models are the most common ones used in commercial CFD applications, the designer should keep in sight that the turbulence model affects the obtained results substantially.

REFERENCES

- [1] Howell, E., "Rockets: A History", space.com contributor, (2015).
- [2] Hammargren, K., "Aerodynamics Modeling of Sounding Rockets", Ms. Thesis, Lulea University of Technology, (2018).
- [3] Guzelbey, I.H., Sumnu, A. and Dogru, M.H., "A Review of Aerodynamic Shape Optimization for a Missile", *The Eurasia Proceedings of Science, Technology, Engineering & Mathematics (EPSTEM)*, 4: 94-102, (2018).
- [4] <https://cpb-us-w2.wpmucdn.com/u.osu.edu/dist/b/38251/files/2018/01/Workshop-1-Aero-and-Propulsion-qsx91h.pdf>, Aerodynamics and Propulsion, Buckeye Space Launch Initiative.
- [5] Cronvich, L.L., "Missile Aerodynamics", *John Hopkins APL Technical Digest*, 175-186, (1983).
- [6] Gönç, L.O., "Computation of External Flow Around Rotating Bodies", *PhD. Thesis*, Middle East Technical University, (2005).
- [7] Baçoğlu, O., "Three Dimensional Aerodynamic Analysis of Missiles by a Panel Method", *MS. Thesis*, Middle East Technical University, (2002).
- [8] Fedaravičius, A., Kılıkevičius, S., Survila, A. and Patašienė, L., "Analysis of Aerodynamic Characteristics of the Rocket-Target for the "Stinger" System", *Problems of Mechatronics Armament, Aviation, Safety Engineering*, 7, 1(23): 7-16, (2016).

- [9] Lopez, D., Dominguez, D. and Gonzalo, J., "Impact of Turbulence Modeling on External Supersonic Flow Field Simulations in Rocket Aerodynamics", *International Journal of Computational Fluid Dynamics*, 27(8-10): 332-341.
- [10] Elliot, J. and Peraire, J., "Practical 3-D Aerodynamic Design and Optimization Using Unstructured Meshes", *AIAA Journal*, 35(9): 1479-1485, (1997).
- [11] Sahu, J. and Heavey, K.R., "Parallel CFD Computations of Projectile Aerodynamics with a Flow Control Mechanism", *Computers & Fluids*, 88: 678-687, (2013).
- [12] Pirzadeh, S.Z. and Frink, N.T., "Assessment of the Unstructured Grid Software TetrUSS for Drag Prediction of the DLR-F4 Configuration", *AIAA*, 2002-0839, (2002).
- [13] Langtry R.B., Kuntz, M. and Menter, F., "Drag prediction of engine air frame interference effects with CFX-5". *Journal of Aircraft*, 42(6): 1523-1529, (2005).
- [14] Kroll N., Rossow, C.C., Schwamborn, D., Becker, K. And Heller, G., "MEGAFLOW-a numerical flow simulation tool for transport aircraft design", *Proceedings of ICAS Congress*, 1105.1-1105.20, (2002).
- [15] Schütte A., Einarsson, G., Madrane, A., Schöning, B., Mönnich, W. and Krüger, W.B., "Numerical simulation of maneuvering aircraft by CFD and flight mechanic coupling", *RTO Symposium*, (2002).